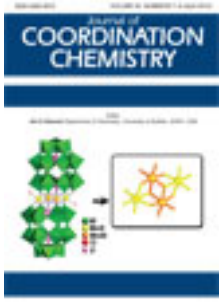

Journal of Coordination Chemistry
Publication details, including instructions for authors and subscription information:
http://www.tandfonline.com/loi/gcoo20

Synthesis of (2E,3E,10E,12E)-3,11-dimethyl-5,9-dioxa-4,10-diazatrideca-3,10-diene-2,12-dione dioxime and its Cu(II), Ni(II), and Co(II) complexes

Serdar Karabocek [a], Ufuk Bayraktar [a], Nevin Karabocek [a], Z. Sibel Sahin [b], Samil Isik [b] & Seda Muhsir [a]

[a] Department of Chemistry, Karadeniz Technical University, 61080 Trabzon, Turkey

[b] Department of Physics, Faculty of Arts and Sciences, Ondokuz Mayis University, Kurupelit, 55139 Samsun, Turkey

Published online: 07 Mar 2012.

To cite this article: Serdar Karabocek, Ufuk Bayraktar, Nevin Karabocek, Z. Sibel Sahin, Samil Isik & Seda Muhsir (2012) Synthesis of (2E,3E,10E,12E)-3,11-dimethyl-5,9-dioxa-4,10-diazatrideca-3,10-diene-2,12-dione dioxime and its Cu(II), Ni(II), and Co(II) complexes, Journal of Coordination Chemistry, 65:7, 1118-1129, DOI: 10.1080/00958972.2012.667564

To link to this article: http://dx.doi.org/10.1080/00958972.2012.667564

Journal of Coordination Chemistry
Vol. 65, No. 7, 10 April 2012, 1118–1129

Synthesis of (2*E*,3*E*,10*E*,12*E*)-3,11-dimethyl-5,9-dioxa-4, 10-diazatrideca-3,10-diene-2,12-dione dioxime and its Cu(II), Ni(II), and Co(II) complexes

SERDAR KARABOCEK*†, UFUK BAYRAKTAR†, NEVIN KARABOCEK†, Z. SIBEL SAHIN‡, SAMIL ISIK‡ and SEDA MUHSIR†

†Department of Chemistry, Karadeniz Technical University, 61080 Trabzon, Turkey
‡Department of Physics, Faculty of Arts and Sciences, Ondokuz Mayis University, Kurupelit, 55139 Samsun, Turkey

(*Received 21 November 2011; in final form 25 January 2012*)

A new tetradentate ligand incorporating dioximes has been synthesized. The dioxime, (H_2L) was characterized by elemental analysis, ^{1}H-NMR, ^{13}C-NMR, IR, and mass spectral data. In addition, its copper(II), nickel(II), and cobalt(II) complexes have been prepared and characterized by physical and spectral methods. Elemental analyses and spectroscopic data of the metal complexes are consistent with the proposed structures. The crystal structure of the Co(II) complex (**7**) was determined by single-crystal X-ray diffraction technique. The inhibitory activities of compounds were examined. Biological activities of the ligand and its metal complexes were tested and the ligand and its metal complexes had inhibitory activity against G(–) *Staphylococcus aureus* and *Pseudomonas aeruginosa*.

Keywords: Dioxime; Cobalt(II) complex; Antimicrobial activity; Crystal structure

1. Introduction

Oximes and oxime ethers are important building blocks in synthesis. Generally, oxime ethers were prepared from *O*-alkyl hydroxylamines and the corresponding aldehydes [1]. The development of high-throughput screening for identification of biologically active compounds is driving the need for combinational libraries of potential ligands. The reaction of an aldehyde or ketone with an oxyamine to form oxime ether is typically quantitative with no side products. Oxime ether formations are chemoselective and tolerant of a wide range of functional groups, including all found in proteins and oligonucleotides. Oxime formation does not require anhydrous conditions, excessive heat, or catalyst and has been demonstrated to form even upon a living cell wall [2]. Both *O*-alkyl oximes and *O*-aryl oximes are stable at physiological pH; *O*-alkyl oximes are also present in a number of approved drugs [3, 4]. One drawback is that while large numbers of aldehydes and ketones are readily available, oxyamine precursors are not.

*Corresponding author. Email: serdar@ktu.edu.tr, serdarkarabocek@gmail.com.tr

Journal of Coordination Chemistry
ISSN 0095-8972 print/ISSN 1029-0389 online © 2012 Taylor & Francis
http://dx.doi.org/10.1080/00958972.2012.667564

Oximes have been widely used as efficient complexing agents in analytical chemistry for isolation, separation, and extraction of different metal ions [5–8]. The incorporation of oxime in multi-donor ligands may give strong chelating agents [6–8]. The α-hydroxy oximes and oxime ethers have received attention as important precursors and intermediates for preparation of a wide variety of natural products, drugs, and metal-binding ligands [9–14]. Furthermore, they can be easily converted into amino alcohols and hydroxy ketones which are very important functional groups [9–14].

This article describes the synthesis and characterization of the new ligand, (2*E*,3*E*,10*E*,12*E*)-3,11-dimethyl-5,9-dioxa-4,10-diazatrideca-3,10-diene-2,12-dione dioxime, (H_2L) and its Cu(II), Ni(II), and Co(II) complexes. The properties of the complexes were investigated by magnetic, physical, and spectral methods. Furthermore, the crystal structure of the Co(II) complex was determined by single-crystal X-ray diffraction.

2. Experimental

2.1. *General*

^{1}H-NMR and ^{13}C-NMR spectra were recorded on a Varian Gemini 200 spectrometer with $CDCl_3$ and DMSO-d_6 as solvents. Chemical shifts (δ) are reported in ppm relative to tetramethylsilane using the solvent signal as internal reference. Elemental analyses (C, H, and N) were performed on a Costech 4010 CHNS Elemental analyzer and metal contents were estimated spectrophotometrically. Infrared (IR) spectra were recorded on an ATI Unicam Matson 1000 Model FTIR spectrophotometer and UV-Vis spectra on an ATI Unicam UV2 Model UV-Vis spectrophotometer. Mass spectra (ESI) were recorded on a Micromass Quanto LC-MS/MS spectrophotometer. The molar conductance was measured with a Metrohm 660 conductivity in DMSO. Room temperature magnetic susceptibility measurements were done on a PAR model 155 vibrating sample magnetometer. All chemicals were of the highest quality available, obtained from local suppliers, and used as received.

2.2. *(3E,10E)-3,11-dimethyl-5,9-dioxa-4,10-diazatrideca-3,10-diene-2,12-dione (3)*

To a vigorously stirring solution of 2,3-butanedione monoxime (2.1 g, 20 mmol) and 1,3-dibromopropane (2.02 g, 10 mmol) in 1 : 1 MeOH/H_2O (25 mL) was added a solution of KOH (1.12 g, 20 mmol) in MeOH (10 mL) at 0°C over *ca* 30 min. After stirring for 24 h at room temperature, the reaction mixture was filtered and the solid washed with MeOH. The crude product was recrystallized from EtOH as a white microcrystalline solid. Yield: 1.9 g (80%), m.p.: 55°C, Ms: (ESI) $m/z = 242$ M^+. Elemental Anal. Calcd ($C_{11}H_{18}N_2O_4$) (%): C, 54.53; H, 7.49; N, 11.56. Found: C, 54.45; H, 7.50; N, 11.60.

2.3. *(2E,3E,10E,12E)-3,11-dimethyl-5,9-dioxa-4,10-diazatrideca-3,10-diene-2,12-dione dioxime (H_2L)*

A solution of (3*E*,10*E*)-3,11-dimethyl-5,9-dioxa-4,10-diazatrideca-3,10-diene-2,12-dione (**3**) (2.4 g, 10 mmol) and $HONH_2 \cdot HCl$ (9.87 g, 142 mmol) in pyridine (50 mL) was

stirred at room temperature for 24 h and the mixture was then poured into ice cold H_2O (200 mL). The resulting precipitate was collected, washed successively with ice cold H_2O and Et_2O, and dried in vacuum over P_2O_5. Recrystallization from 1 : 1 EtOH/DMSO (30 cm^3) gave (H_2L) as a colorless microcrystalline solid. Yield: 2.4 g (88%), m.p.: 150–155°C, Ms: (ESI) $m/z = 272$ M^+. Elemental Anal. Calcd ($C_{11}H_{20}N_4O_4$) (%): C, 48.50; H, 7.40; N, 20.58. Found: C, 48.60; H, 7.35; N, 20.65.

2.4. *Synthesis of metal complexes*

A solution of metal salts (1 mmol) in Me_2CO (20 mL) was added to the ligand (270 mg, 1 mmol) in Me_2CO (20 mL) and the mixture was refluxed with stirring for 10 h. The product was filtered off and washed with H_2O, MeOH, and Et_2O and dried over P_2O_5. Recrystallization from 1 : 1 EtOH/DMSO (25 mL) gave the products.

2.4.1. [Cu(H_2L)(ClO_4)$_2$] (5). Yield 365 mg (70%) as a brown microcrystalline solid. Anal. Calcd for $C_{11}H_{20}Cl_2N_4O_{12}Cu$ (%): C, 24.70; H, 3.77; N, 10.48; Cu, 11.88. Found (%): C, 24.80; H, 3.85; N, 10.45; Cu, 11.75. ESI MS $m/z = 334.85$ M^+.

2.4.2. [Ni(H_2L)(ClO_4)$_2$] (6). Yield 330 mg (60%) as a pale-red microcrystalline solid. Anal. Calcd for $C_{11}H_{20}Cl_2N_4O_{12}Ni$ (%): C, 24.90; H, 3.80; N, 13.40; Ni, 11.1. Found (%): C, 25.0; H, 3.75; N, 13.47; Ni, 11.05. ESI MS $m/z = 329.87$ M^+.

2.4.3. [Co(H_2L)Cl_2] (7). Yield 300 mg (75%) as deep-brown crystalline solid. Anal. Calcd for $C_{11}H_{20}Cl_2N_4O_4Co$ (%): C, 32.85; H, 5.0; N, 13.90; Co, 14.65. Found (%): C, 32.90; H, 4.95; N, 13.95; Co, 14.70. ESI MS $m/z = 402$ M^+.

2.5. *Antibacterial activity test*

The antibacterial activities of the ligand and complexes *in vitro* have been tested by the paper disc diffusion method [15]. The chosen strains were G(+) *Staphylococcus aureus*, G(–) *Escherichia coli*, and G(–) *Pseudomonas aeruginosa*. The ligand and its metal complexes dissolved in DMSO were first diluted to 1000 μg mL^{-1}, and then serial, two-fold dilutions were made in a concentration range from 10 to 1000 μg mL^{-1} in 10 mL sterile test tubes containing nutrient broth. The plates were prepared by adding 100 μL of nutrient broth and 10, 14, 16, 20, 22 μL, respectively, of the inoculum into each well. Nutrient agar was poured onto a plate and allowed to solidify. The liquid medium containing the bacterial subcultures was autoclaved before inoculation. The bacteria were then cultured for 24 h at 37°C in an incubator. Bacterial strains were inoculated onto the medium plates with absorbent cotton and 10 μL of the test compounds (DMSO solutions) were added dropwise to a 6 diameter filter paper disc placed at the center of each agar plate. The plates were kept at 5°C for 1 h and then transferred to an incubator maintained at 37°C. The width of the growth inhibition zone around the disc was measured after 24 h incubation. Four replicas were made for each test. The tolerance limit of error is not more than ±2. DMSO impregnated discs were used as

negative control. *Ampicillin* was used as positive standard to determine the sensitivity of one strain/isolate in each microbial species tested.

2.6. *X-ray crystallography*

Intensity data of **7** were collected using a STOE IPDS II diffractometer with graphite-monochromated Mo-Kα radiation (λ = 0.71073) at 296 K. Data reduction and numerical absorption correction were performed using the X-RED program [16]. The structure was solved by direct-methods using SHELXS-97 and refined by full-matrix least-squares on F^2 using SHELXL-97 [17] from within the WINGX [18] suite of software. All non-hydrogen atoms were found from the difference Fourier map and refined anisotropically. Hydrogen atoms bonded to carbon were refined using a riding model, with C–H = 0.96–0.97 Å. The constraint $U_{iso}(H) = 1.2U_{eq}$ (methylene C) or $1.5U_{eq}$ (methyl C) was applied. H_2 and H_3 were located in difference map and refined freely with occupancy factors of 0.60(5) and 0.40(5), respectively. Molecular diagram was created using ORTEP-III [19]. Geometric calculations were performed with PLATON [20]. The crystal data are summarized in table 1 with details about data collection and refinement.

3. Results and discussions

(2*E*,3*E*,10*E*,12*E*)-3,11-dimethyl-5,9-dioxa-4,10-diazatrideca-3,10-diene-2,12-dione dioxime, (H_2L) was synthesized in pyridine by reaction of (3*E*,10*E*)-3,11-dimethyl-5,

Table 1. Crystal data and structure refinement details for **7**.

Empirical formula	$C_{11}H_{19}Cl_2CoN_4O_4$
Formula weight	401.13
Crystal system	Monoclinic
Space group	$P2_1/c$
Unit cell dimensions (Å,°)	
a	9.6602(6)
b	11.7780(5)
c	15.0879(9)
β	90
Volume (Å^3), *Z*	1612.64(15), 4
Calculated density (g cm^{-3})	1.652
Absorption coefficient (mm^{-1})	1.42
F(000)	824
Crystal size (mm^3)	0.44 × 0.34 × 0.26
θ range for data collection (°)	2.3–27.8
Limiting indices	$-12 \le h \le 11$; $-15 \le k \le 15$; $-19 \le l \le 19$
Reflections collected	10,103
Independent reflection	3760
Absorption correction	Numerical
Data/parameters/restraints	3760/210/0
Goodness-of-fit on F^2	0.94
R_1/wR_2 [$I > 2\sigma(I)$]	0.029/0.072
R_1/wR_2 (all data)	0.040/0.069
Largest difference peak and hole (e Å^{-3})	0.21 and −0.58

9-dioxa-4,10-diazatrideca-3,10-diene-2,12-dione (**3**) with hydroxylamine hydrochloride. The dioxime (H_2L) and dione (**3**) were characterized by elemental analysis, ^{1}H-NMR, ^{13}C-NMR, IR, and mass spectral data. Copper(II), nickel(II), and cobalt(II) complexes of dioxime have been prepared and characterized by elemental analyses and magnetic moments, UV-Vis, IR, and mass spectral data. In the proposed structure of (H_2L), N_4 units are available for the complexation of metal ions in square-planar coordination geometry.

3.1. *NMR spectra*

^{1}H-NMR spectrum of dioxime has been recorded in DMSO-d_6. The ^{1}H-NMR spectrum of dione (**3**) has been recorded in $CDCl_3$ solution. The ^{1}H-NMR spectrum of **3** shows a singlet at 2.35 ppm (CH_3-1, 6H), 1.85 ppm (CH_3-4, 6H) for the presence of methyl protons. The methylene protons are a triplet at 4.40 ppm (CH_3-5, 4H) and a multiplet at 2.20 ppm (CH_3-6, 2H). ^{1}H-NMR spectrum of dioxime shows a singlet at 1.94 ppm (CH_3-1, 6H) and 1.89 ppm (CH_3-4, 6H) for methyls. The methylene protons are a triplet at 4.16 ppm (CH_3-5, 4H) and a multiplet at 1.90 ppm (CH_3-6, 2H). In the ^{1}H-NMR spectrum, methyl (CH_3-1, CH_3-4) and methylene (CH_2-6) of dioxime overlapped (table 2). The oxime OH is a singlet at 11.56 ppm. The ^{13}C-NMR spectrum of dioxime ligand shows six different signals; methyl and methylene carbon appear at 10–22 ppm and the azomethine (C=N) carbon at 153–154 ppm.

3.2. *Mass spectra*

Mass spectra of all compounds were recorded in pyridine. The mass spectra (ESI) exhibit the molecular ion at $m/z = 242$ M^+ for **3** and $m/z = 272$ M^+ for H_2L, which indicates formation of the dione and dioxime. The molecular ion peak of Co(II) complex $[Co(H_2L)Cl_2]$ is at (m/z, ESI) 402 M^+. In mass spectra of the Cu(II) complex m/z 334.85 ($[HLCu]^+$, Calcd 334.84 amu) represents the molecular ion of the Cu(II) complex with 15% abundance. The other peaks (302, 278, 200, 102, and 75) are attributed to fragmentation. In a similar way the mass spectrum of the Ni(II) complex was observed at m/z 329.87 ($[HLNi]^+$, Calcd 329.99 amu) for the molecular ion peak with 19% abundance. The other peaks (296, 273, 200, 102, and 75) in the mass spectrum are attributed to the fragmentation. The base peak is observed at m/z 102.09 (100% abundance). In mass spectra of the Cu(II) and Ni(II) complexes perchlorate was not observed. From the data we conclude that the molecular weight was in good agreement with the calculated molecular weight of ligand and its metal complexes. Schemes 1 and 2 demonstrate the proposed path of decomposition for the investigated Cu(II) and Ni(II) complexes. The mass spectra show formation of the ligand and its metal complexes.

Table 2. ^{1}H-NMR data of dione (**3**) and ligand (**4**).

Compound	CH_3-1	CH_3-4	$-CH_2$-5	$-CH_2$-6	$-$OH
3	2.35(s, 6H)	1.85(s, 6H)	4.40(t, 2H)	2.20(q, 4H)	–
H_2L (**4**)	1.94(s, 6H)	1.89(s, 6H)	4.16(t, 2H)	1.90(q, 4H)	11.56(s, 2H)

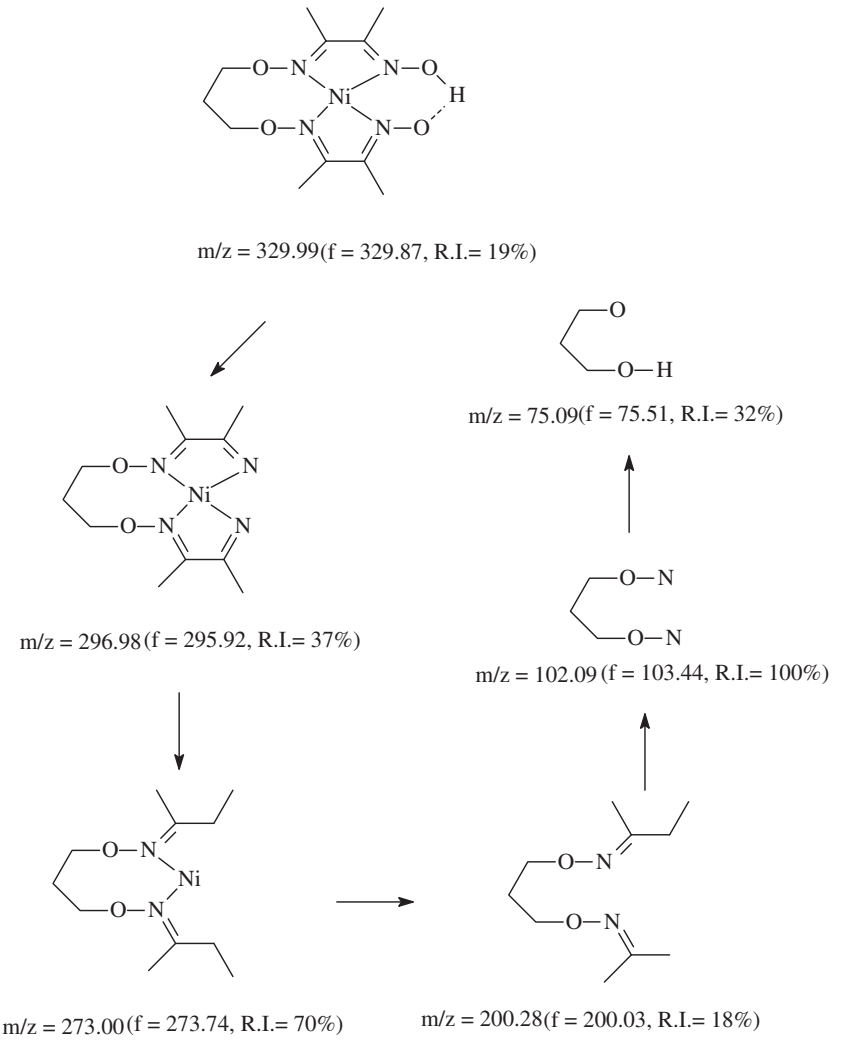

Scheme 1. Mass fragmentation pattern of the Ni(II) complex of dioxime. m/z = ratio of mass to charge (calculated); f = found value of m/z; R.I. = relative intensity of the peak.

3.3. *IR spectra*

Table 3 gives the main IR absorptions of the ligand and complexes. Certain bands in IR spectra were used to establish the nature of the complexes. The strong band at 1605 cm^{-1} is assigned to ν(C=N) [21]. In the IR spectrum of H_2L^1 a band for ν(O–H) at 3240 cm^{-1} was observed. The perchlorate complex shows a doublet at 1020–1095 cm^{-1}, due to splitting of the [$\nu(T_2)$] vibration into [ν_3(A)] and [ν_3(E)]. The presence of these bands shows perchlorate is coordinated in the Cu(II) and Ni(II) complexes [22]. Finally, peaks appearing between 460 and 478 cm^{-1} are attributed to ν(N–M–N) [22]. A strong band at *ca* 1605 cm^{-1}, which shifts by 5–15 cm^{-1} to lower frequency upon coordination, is assigned to ν(C=N). Significant shifts in ν(C=N) upon complexation support coordination of the ligand through the oxime nitrogen.

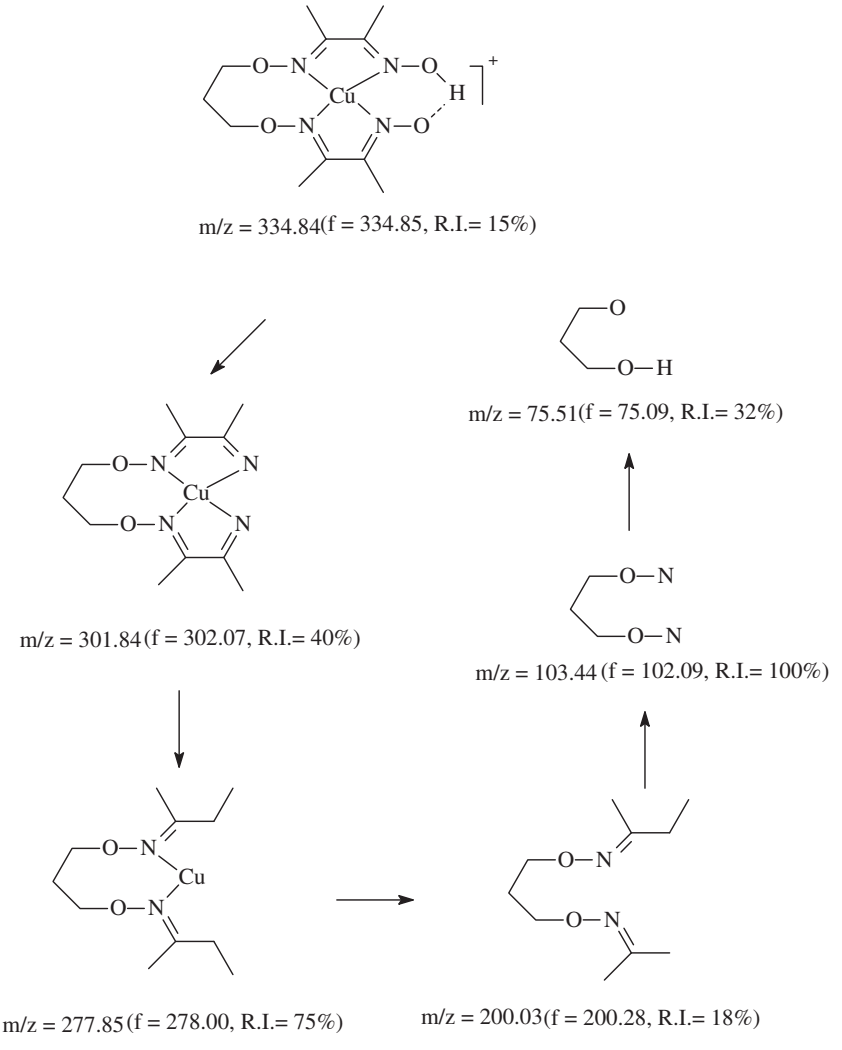

Scheme 2. Mass fragmentation pattern of the Cu(II) complex of dioxime. m/z = ratio of mass to charge (calculated); f = found value of m/z; R.I. = relative intensity of the peak.

Table 3. Characteristic IR bands of the ligand and its metal complexes (cm^{-1}).

Compound	ν(O–H)	ν(C=O)	ν(C=N)	ν(N–M–N)	$\nu(ClO_4)$
3	–	1692	1605	–	–
H_2L	3240	–	1600	–	–
$[Cu(H_2L)(ClO_4)_2]$	3225	–	1590	460	1093, 1023 (d)
$[Ni(H_2L)(ClO_4)_2]$	3230	–	1594	440	1095, 1020 (d)
$[Co(H_2L)Cl_2]$	3200	–	1602	478	–

Table 4. Physical data of the ligand and its metal complexes.

Compound	Color	μ_{eff} [a]	Yield	d–d (cm^{-1}*)
3	White	–	80	–
H_2L	White	–	88	–
$[Cu(H_2L)(ClO_4)_2]$	Brown	1.80	70	13,480, 15,550, 25,850
$[Ni(H_2L)(ClO_4)_2]$	Pale-red	2.90	60	12,700, 17,950, 25,150
$[Co(H_2L)Cl_2]$	Deep-brown	4.65	75	11,300, 17,800, 24,500

[a]Per metal atom at 297 K (B.M.).
*UV-Vis spectra were recorded in DMSO.

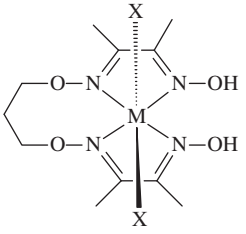

X= ClO_4^-, Cl^-
M= Cu(II) (5), Ni(II) (6), Co(II) (7)

Figure 1. Proposed structures for the metal complexes.

3.4. *Magnetic properties and electronic absorption spectra*

Electronic spectra of the complexes were recorded in DMSO (ε in L $mol^{-1}\,cm^{-1}$). The electronic spectrum of **5** shows bands at 13,480(725), 15,550(605), and 25,850(360) cm^{-1}, assignable to a $^2E_g \rightarrow {}^2T_{2g}$ transition and charge transfer (table 4). Electronic spectral data coupled with magnetic moment of 1.80 B.M. for Cu(II) complexes suggests octahedral geometry (figure 1) [23]. Ni(II) complex displays bands at 12,700(1010), 17,950(590), and 25,150(355) cm^{-1} assignable to $^3A_{2g} \rightarrow {}^3T_{2g}(F)$, $^3A_{2g} \rightarrow {}^3T_{1g}(F)$, and $^3A_{2g} \rightarrow {}^3T_{1g}(P)$, respectively. These electronic transitions along with magnetic moment of 2.90 B.M. suggest octahedral geometry for Ni(II) complex [24]. The Co(II) complex shows three bands at 11,300(950), 17,800(515), and 24,500(450) cm^{-1} assignable to $^4T_{1g}(F) \rightarrow {}^4T_{1g}(P)$, $^4T_{1g}(F) \rightarrow {}^4A_{2g}$, and $^4T_{1g}(F) \rightarrow {}^4T_{1g}(P)$ transitions, respectively. These transitions and observed magnetic moment of 4.65 B.M. indicate high spin octahedral complex (figure 1) [24–26]. The calculated values of ligand field splitting energy ($10\,D_q$), Racah interelectronic repulsion parameter (β), covalent factor (β), ratio ν_2/ν_1, and ligand field stabilization energy (LFSE), given in table 5, support the proposed geometry for all the complexes.

3.5. *Antimicrobial activity*

Measuring the bacteriostatic diameter can test the susceptibility of a bacterium toward a drug. The antibacterial activities *in vitro* are shown in table 6 for 0.1 and 0.22 μg mL^{-1} solutions of the ligand and metal complexes. No inhibitor activity against G(–) *E. coli*

Table 5. Ligand field parameter of the complexes.

Complex	Ligand field splitting energy (D_q cm^{-1})	Racah interelectronic repulsion parameter (B cm^{-1})	Covalent factor (β)	β (%)	ν_2/ν_1	LFSE (kcal mol^{-1})
$[Cu(H_2L)(ClO_4)_2]$	13,480	96.06	–	–	–	38.50
$[Ni(H_2L)(ClO_4)_2]$	12,700	843.6	0.8115	23.45	1.40	36.28
$[Co(H_2L)Cl_2]$	11,300	914.0	0.9425	6.25	1.57	32.28

Table 6. Antibacterial activity data for H_2L and its metal complexes.

Compound	μg mL^{-1}	Average value of bacteriostatic diameter (mm)		
		E. coli	*S. aureus*	*P. aeruginosa*
H_2L	0.10	7.0	7.0	7.0
	0.14	7.0	7.2	7.4
	0.16	7.0	7.7	7.9
	0.20	7.0	8.0	8.0
	0.22	7.0	8.0	8.0
$[Cu(H_2L)(ClO_4)_2]$	0.10	7.0	7.0	9.0
	0.14	7.0	7.5	7.0
	0.18	7.0	8.7	7.0
	0.20	7.0	9.0	7.0
	0.22	7.0	9.0	7.0
$[Ni(H_2L)(ClO_4)_2]$	0.10	7.0	7.0	10.0
	0.14	7.0	7.8	9.0
	0.18	7.0	9.7	8.3
	0.20	7.0	10.0	8.0
	0.22	7.0	10.1	8.0
$[Co(H_2L)Cl_2]$	0.10	7.0	7.0	9.0
	0.14	7.0	7.4	8.4
	0.18	7.0	7.9	8.1
	0.20	7.0	8.0	8.0
	0.22	7.0	8.1	8.1
$Cu(ClO_4)_2$	0.10	7.0	7.0	7.0
	0.14	7.0	7.0.	7.4
	0.18	7.0	7.2	7.5
	0.20	7.0	7.2	7.5
	0.22	7.0	7.2	7.5
$Ni(ClO_4)_2$	0.10	7.0	7.0	7.0
	0.14	7.0	7.3	7.1
	0.18	7.0	7.4	7.1
	0.20	7.0	7.5	7.2
	0.22	7.0	7.5	7.2
$CoCl_2$	0.10	7.0	6.9	7.0
	0.14	7.0	6.9	7.1
	0.18	7.0	7.0	7.2
	0.20	7.0	7.0	7.3
	0.22	7.0	7.0	7.3
Ampicillin	0.10	10	15	12
	0.14	10	17	12
	0.18	10	17	12
	0.20	10	17	12
DMSO	–	NA	NA	NA

NA, not active.

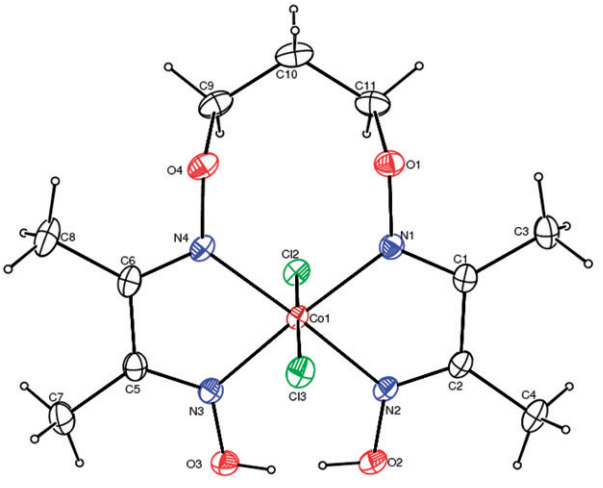

Figure 2. A view of the molecular structure of **7** showing the atom-numbering scheme. Displacement ellipsoids are drawn at the 30% probability level and hydrogen atoms are shown as small spheres of arbitrary radii.

Table 7. Selected bond lengths (Å) and angles (°) for **7**.

Co1–Cl2	2.2360(5)	Co1–N1	1.9211(14)
Co1–Cl3	2.2404(5)	Co1–N2	1.9050(14)
Co1–N3	1.9120(15)	Co1–N4	1.9203(14)
C1–N1	1.290(2)	C2–N2	1.291(2)
C6–N4	1.289(2)	C5–N3	1.300(2)
N2–Co1–N3	96.92(7)	N2–Co1–N4	176.91(6)
N3–Co1–N4	80.05(6)	N2–Co1–N1	79.86(6)
N3–Co1–N1	176.73(6)	N4–Co1–N1	103.17(6)
N2–Co1–Cl2	90.03(5)	N3–Co1–Cl2	89.48(5)
N4–Co1–Cl2	90.54(5)	N1–Co1–Cl2	91.05(5)
N2–Co1–Cl3	88.60(5)	N3–Co1–Cl3	90.06(5)
N4–Co1–Cl3	90.80(5)	N1–Co1–Cl3	89.33(5)
Cl2–Co1–Cl3	178.49(2)		

was observed. The ligand and its metal complexes had inhibitory activity against G(–) *S. aureus* and *P. aeruginosa*. As the concentration was increased to 0.2 μg mL^{-1}, the biological activity of the metal complexes against G(–) *P. aeruginosa* was decreased. The inhibitor activities of the metal complexes against other strains are currently being tested. Antibacterial activities of the ligand and its metal complexes were found to be lower than *ampicillin* (table 6).

3.6. *Crystal structure of [Co(H$_2$L)Cl$_2$] (7)*

The molecular structure of **7** with atom labeling is shown in figure 2. Selected bond lengths and angles are listed in table 7. The local structure around Co(II) is that of a distorted octahedron, of which the equatorial plane is formed by four nitrogen

Table 8. Hydrogen-bonding geometry for **7**.

D–H···A	D–H (Å)	H···A (Å)	D···A (Å)	D–H···A (°)
C11–H11A···Cl2	0.97	2.83	3.615(2)	139
O2–H2···N3	0.84(6)	2.26(5)	2.958(2)	141(4)
O2–H2···O3	0.84(6)	1.62(6)	2.450(2)	174(4)
O3–H3···N2	0.78(9)	2.36(8)	2.961(2)	135(6)
O3–H3···O2	0.78(9)	1.69(9)	2.450(2)	167(7)
C3–H3A···O3^{i}	0.96	2.47	3.320(3)	148
C3–H3B···Cl3^{ii}	0.96	2.80	3.654(2)	149

Symmetry codes: $^{i}x, -y+3/2, z+1/2$; $^{ii}-x+1, y-1/2, -z+1/2$.

atoms of H_2L. The axial positions in the octahedron are occupied by two chlorides. The angles at Co1 involving *cis*-donors lie in the range 79.86(6)–103.17(6)°, while *trans* angles of 176.73(6)° and 178.49(2)° are observed. The Co–N and Co–Cl bond lengths are normal (table 7) and are comparable with the corresponding values observed in a related complex [27–29]. The bond lengths of N = C are within the range 1.289(2)–1.300(2) Å and similar to those of the previously reported structures [28, 29]. Complex **7** has two chelate ring types. In the first of these, N1 and N2 are bonded to Co1, thus generating a five-membered chelate ring (C1/C2/N2/Co1/N1). Similarly, N3 and N4 are bonded to Co1, generating a five-membered chelate ring (C5/C6/N4/Co1/N3). These chelate rings are approximately planar, with maximum deviations from the least-squares planes being 0.0261(10) Å for N2 and 0.0189(10) Å for N3. In the other type, N1 and N4 are bonded to Co1, generating an eight-membered chelate ring (N1/O1/C11/C10/C9/O4/N4/Co1).

Within the asymmetric unit, intramolecular C–H···Cl and O–H···N hydrogen bonds define S(5) and S(6) motifs [30]. Compound **7** also contains two intermolecular hydrogen bonds. In the first, C3 at (x, y, z) acts as a hydrogen-bond donor, *via* H3A, to O3 at $(x, -y+3/2, z+1/2)$, forming a C(7) chain running parallel to the [001] direction. In the second, C3 at (x, y, z) acts as a hydrogen-bond donor, *via* H3B, to Cl3 at $(-x+1, y-1/2, -z+1/2)$, forming a C(6) chain running parallel to the [010] direction. The combination of the C(6) and C(7) chains generates a chain of edge-fused $R_4^4(14)$ rings parallel to the *bc* plane. Details of these interactions are given in table 8.

Oxime ethers are important sub-structures of biologically active compounds used extensively by the pharmaceutical and agrochemical industries [2]. They are useful motifs with which to introduce diversity and to create large libraries of compounds.

Supplementary material

CCDC 817156 contains the supplementary crystallographic data for this article. This data can be obtained free of charge *via* http://www.ccdc.cam.ac.uk/conts/retrieving.html, or from the Cambridge Crystallographic Data Centre, 12 Union Road, Cambridge CB2 1EZ, UK; Fax: (+44) 1223-336-033; or E-mail: deposit@ccdc.cam.ac.uk.

Acknowledgments

This work was supported by Karadeniz Technical University Research Fund, and its project code is 2005.111.02.2.

References

[1] K. Serbest, I. Değirmencioglu, S. Karaböcek, S. Güner. *Transition Met. Chem.*, **26**, 232 (2001).
[2] G.A. Lemieux, K.J. Yarema, C.L. Jacobs, C.R. Bertozzi. *J. Am. Chem. Soc.*, **121**, 4278 (1999).
[3] V.A. Polyakov, M.I. Nelen, N. Nazarpack-Kandlousy, A.D. Ryabox, A.V. Eliseev. *J. Phys. Org. Chem.*, **12**, 357 (1999).
[4] M.I. Wilde, G.L. Plasker, P. Benfield. *Drugs*, **46**, 895 (1993).
[5] M.S. Ray, G. Mukhopadhyay, R. Bhattacharya, S. Chaudhuri, L. Righi, G. Bocelli, A. Ghosh. *Polyhedron*, **22**, 617 (2003).
[6] S. Chattopadhyay, M.S. Ray, S. Chaudhuri, G. Mukhopadhyay, G. Bocelli, A. Cantoni, A. Ghosh. *Inorg. Chim. Acta*, **359**, 1367 (2006).
[7] M.S. Ray, A. Ghosh, R. Bhattacharya, G. Mukhopadhyay, M.G.B. Drew, J. Ribas. *Dalton Trans.*, 252 (2004).
[8] M.S. Ray, A. Ghosh, S. Chaudhuri, M.G.B. Drew, J. Ribas. *Eur. J. Inorg. Chem.*, 3110 (2004).
[9] M. Shimizu, K. Tsukamoto, T. Fujisawa. *Tetrahedron Lett.*, **38**, 5193 (1997).
[10] J.A. Marco, M. Carda, F. Murga, F. Conzalez, E. Falomir. *Tetrahedron Lett.*, **38**, 1841 (1997).
[11] J.A. Marco, M. Carda, J. Murga, S. Rodriguez, E. Falomir, M. Olive. *Tetrahedron: Asymmetry*, **9**, 1679 (1998).
[12] K.C. Nicolaou, H.J. Mitchell, F.L. van Delft, F. Rubsam, R.M. Rodriguez. *Angew. Chem. Int. Ed.*, **37**, 1871 (1998).
[13] S.C. Bergmeier. *Tetrahedron*, **56**, 2561 (2000).
[14] M. Periasamy. *Pure Appl. Chem.*, **68**, 663 (1996).
[15] D. Liu, K. Kwasniewska. *Bull. Environ. Contam. Toxicol.*, **27**, 289 (1981).
[16] Stoe & Cie. *X-RED32 (Version 1.04)*, Stoe & Cie, Darmstadt, Germany (2002).
[17] G.M. Sheldrick. *Acta Crystallogr.*, **A64**, 112 (2008).
[18] L.J. Farrugia. *WINGX-A Windows Program for Crystal Structure Analysis*, University of Glasgow (1998).
[19] L.J. Farrugia. *Appl. Crystallogr.*, **30**, 565 (1997).
[20] A.L. Spek. *PLATON-A Multipurpose Crystallographic Tool*, Utrecht University, Utrecht, The Netherlands (2005).
[21] K. Serbest, A. Colak, S. Guner, S. Karaböcek. *Transition Met. Chem.*, **26**, 625 (2001).
[22] Y.S. Sharma, H.N. Pandey, P. Mathur. *Polyhedron*, **13**, 3111 (1994).
[23] G.L. Eichhorn, J.C. Bailar. *J. Am. Chem. Soc.*, **75**, 2905 (1953).
[24] A.B.P. Lever. *Inorganic Electronic Spectroscopy*, pp. 275–361, Elsevier, Amsterdam (1968).
[25] F.A. Cotton, G. Wilkinson. *Advanced Inorganic Chemistry*, 5th Edn, Wiley, New York (1988).
[26] F. Firdos, K. Fatima, A. Khan. *J. Serb. Chem. Soc.*, **74**, 939 (2009).
[27] S. Martin, C. Revathi, A. Dayalan. *J. Chem. Crystallogr.*, **39**, 908 (2009).
[28] P. Ramesh, A. Subbiahpandi, P. Jothi, C. Revathi, A. Dayalan. *Acta Cryst.*, **E64**, m300 (2008).
[29] X.-J. Shen, L.-P. Xiao, R.-R. Xu. *Acta Cryst.*, **E61**, m1185 (2005).
[30] J. Bernstein, R.-E. Davis, L. Shimoni, N.-L. Chang. *Angew. Chem. Int. Ed. Engl.*, **34**, 1555 (1973).